Takada and Dupuis' r(C–C) = 1.388 Å and r(C–H) = 1.075 Å, we calculate effective X–Y bond lengths (r_0) of 1.505 Å (CH_2CHCH_2), 1.555 Å (CH_2CDCH_2), and 1.612 Å (CD_2CDCD_2). The vibrational frequencies in the neutral molecules are the experimental values from this experiment. The frequencies for the anions were varied along with the X–Y–X angle to obtain the best fit to our fitted FCF's.

Our best fit to the experimental FCF's was for a bond angle change of 16° with a bending frequency in the anion ($CH_2CHCH_2^-$) of about 500 cm^{-1}. The optimal fit is insensitive to the ion frequency; the bond angle changes by one degree or less across a large range of frequencies. The calculated results for the three isomers are reported in Table V. We conclude that the bond angle change between allyl anion and allyl is 16 ± 4°. We feel an uncertainty of 4° is generous even considering that we have assumed a harmonic oscillator and ignored the bond strength contribution to the bend. If one uses the calculated C–C–C angle for CH_2CHCH_2 from Takada and Dupuis of 124°, then the C–C–C angle is 140 ± 4° for $CH_2CHCH_2^-$. Note that this is not a unique answer because a bond angle decrease of 16° works equally well. We believe that the angle increases, however, because the detached electron is from an orbital which is antibonding between the terminal carbons.[33] An increasing angle is consistent with previous calculations.[31-33,40,41]

Synthesized spectra based on our calculated FCF's for the three isotopes are presented in Figure 9. One immediately notices that we have fit the data (Figures 3–5) quite well in all three cases for the first four or five peaks. For the higher vibrational states this simple model does not fit the data well at all. Note that this is also the spectral region where the peak widths seem to become larger. It is clear that something unexpected is happening in these higher levels. We do not know what this effect is, but we remind the reader that all the peaks in the absorption spectrum of allyl[25] were broadened by predissociation. This phenomenon warrants further study.

Conclusion

The allyl anion ($CH_2CHCH_2^-$) and two isotopically substituted species ($CH_2CDCH_2^-$ and $CD_2CDCD_2^-$) have been studied in negative ion photoelectron spectroscopy. The electron affinities of these three radicals as well as the heat of formation of the allyl anion ($CH_2CHCH_2^-$) are collected in Table II. The values are in fairly good agreement with previous gas-phase ion chemistry studies.[6-8]

The photoelectron spectra we observe show excitation in only one vibronic mode to be important. We identify this mode as the in-plane skeletal bend of the allyl radical. The vibrational frequencies are reported in Table III. We conclude that the major geometry change occurring when an electron is added to ground-state allyl radical is an opening in the C–C–C bond angle. A Franck–Condon analysis of our experimental peak intensities is performed. We find this bond angle to increase by about 16°.

Acknowledgment. We would like to acknowledge stimulating conversations with Larry Harding, Tony Rappe, Wes Borden, and Veronica Bierbaum. This work was supported by the United States Department of Energy (Contract DE-AC02-80ER10722).

(40) S. D. Peyerimhoff and R. J. Buenker, *J. Chem. Phys.*, **51**, 2528 (1969).
(41) S. D. Peyerimhoff and R. J. Buenker, *Theor. Chim. Acta*, **24**, 132 (1972).

Resonance Raman Studies of O_2 Stretching Vibrations in Oxygen Adducts of Cobalt Porphyrins. The Importance of Vibrational Coupling

Krzysztof Bajdor, James R. Kincaid,* and Kazuo Nakamoto*

Contribution from the Todd Wehr Chemistry Building, Marquette University, Milwaukee, Wisconsin 53233. *Received November 17, 1983*

Abstract: Studies are undertaken to examine the role of vibrational coupling in determining the $\nu(O_2)$ frequencies of molecular oxygen adducts of cobalt porphyrin complexes with a number of axial ligands. Specifically, we have carried out strategic isotopic labeling in order to demonstrate that multiple bands and shifts of $\nu(O_2)$ may arise from vibrational coupling and thus to distinguish this effect from other, steric or environmental, factors that may give rise to such behavior. Strong evidence is presented for vibrational coupling between $\nu(O_2)$ and internal modes of axial ligands that occur at comparable frequencies. The utility of mixed-isotope (^{16}O–^{18}O) experiments for detecting vibrational coupling is explored. Results, using a limited number of axial ligands (pyridine and imidazole and various substituted analogues) and several different cobalt porphyrins (tetraphenylporphine, octaethylporphine, protoporphyrin IX and diformyl deuteroporphyrin IX dimethyl esters, and picket-fence porphyrin), indicate that axial and (relatively weak) equatorial electronic effects on $\nu(O_2)$ are consistent with stabilization of charge separation in the $Co^{\delta+}$–$O_2^{\delta-}$ formulation. Also, relatively large effects on the $\nu(O_2)$ frequency are brought about by interactions of bound O_2 with solvent molecules (e.g., methylene chloride and methanol).

Introduction

The nature of dioxygen binding to myoglobin and hemoglobin has been an intensively investigated subject[1-3] during the past decade, and many model systems that reversibly bind molecular oxygen have been developed in an effort to understand the steric and electronic factors which control oxygen binding in the native proteins. These model systems include the "picket-fence",[4,5] "chelated",[6] "capped",[7,8] "strapped",[9] and "basket-handle"[10] me-

(1) Valentine, J. S. *Chem. Rev.* **1973**, *73*, 235.
(2) Wayland, B. B.; Minkiewiez, J. V.; Abd-Elmazeed, M. E. *J. Am. Chem. Soc.* **1974**, *96*, 2795.
(3) Jones, R. D.; Summerville, D. A.; Basolo, F. *Chem. Rev.* **1979**, *79*, 139.
(4) Collman, J. P.; Gagne, R. R.; Reed, C. A.; Halbert, T. R.; Lang, G.; Robinson, W. T. *J. Am. Chem. Soc.* **1975**, *97*, 1427.
(5) Collman, J. P.; Halbert, T. R.; Suslick, K. S. In "Metal Ions in Biology"; Spiro, T. G., Ed.; John Wiley: New York, 1980; Vol. 2, p 1.

0002-7863/84/1506-7741$01.50/0 © 1984 American Chemical Society

talloporphyrins. Ideally, the spectroscopic and functional response to controlled structural perturbations in the model systems may be related to the corresponding properties of the native systems. In order to make most effective use of such model compounds, it is important to establish reliable spectroscopic probes of the key structural elements in the models and native systems, especially the metal–oxygen groups.

Historically, vibrational spectroscopy offers great potential for detection of slight alterations in bonding associated with minor structural perturbations. Unfortunately, in the case of myoglobin and hemoglobin and relevant model systems this potential has not been fully realized since much confusion remains regarding the identification and behavior of the O–O stretching vibration of bound molecular oxygen. The ν(O–O) in oxymyoglobin (oxyMb) and oxyhemoglobin (oxyHb) were first reported by Caughey et al.[11] at 1103 cm^{-1} and 1107 cm^{-1}, respectively, from infrared data. The ν(Fe–O) in oxyHb was first observed by Brunner[12] at 567 cm^{-1} using resonance Raman (RR) spectroscopy. Although a virtually identical frequency (568 cm^{-1}) was observed for the oxy (iron picket-fence porphyrin) by Burke et al.,[13] the ν(O–O) for this model system had been observed in the infrared (IR) spectrum by Collman et al.[14] at 1163 cm^{-1}, a value which is substantially different from those observed in the proteins. Soon after this, Alben et al.[15] observed another band at 1156 cm^{-1} in the IR spectrum of oxyHb and proposed that the observation of two IR bands at 1156 and 1107 cm^{-1} results from Fermi resonance involving the first overtone of ν(Fe–O) at 567 cm^{-1}.

Resonance Raman spectroscopy is not a useful probe of ν(O–O) in the iron model compounds or native proteins since this mode is not enhanced by laser lines that have been used thus far,[16] an observation in agreement with the results of MO calculations by Karplus and co-workers[17] which predict the Fe–O_2 charge transfer (CT) transition of oxyHb to be in the range of 780–1300 nm. On the other hand, strong enhancement of both ν(Co–O) and ν(O–O) has been observed in the case of oxyCoMb and oxyCoHb[18] (with 406.7 nm) and cobalt model systems[19] (with 457.9 nm). Presumably, this enhancement originates via resonance with an apparent out-of-plane charge-transfer transition of the type $\pi^*(\pi^*_g O_2/d_{xz}Co) \rightarrow \sigma^*(d_{z^2}Co/\pi^*_g O_2)$[17,18] which is near the Soret transition.

Somewhat surprisingly, multiple bands were also observed in the cobalt-substituted protein systems by Tsubaki and Yu,[18] who detected three isotope ($^{16}O_2/^{18}O_2$) sensitive bands at 1103, 1137, and 1153 cm^{-1} in the RR spectrum of CoMb-$^{16}O_2$. Corresponding bands were observed at 1107, 1137, and 1152 cm^{-1} in the spectrum of CoHb-$^{16}O_2$. These workers interpreted this behavior to result from a type of resonance interaction between one ν(O–O) at ~1122 cm^{-1} and an accidentally degenerate porphyrin ring mode at 1123 cm^{-1} (giving rise to the bands observed at 1137 and 1103 cm^{-1}) and one other, unperturbed, ν(O–O) at 1153 cm^{-1}. Yu and co-workers suggested that the former may originate in a species in which the bound oxygen is hydrogen bonded to the distal histidine thus lowering its ν(O–O) whereas the latter is due to the O_2 that is rotated by 40° around the N(proximal histidine)–Co–O axis relative to the other O_2 and thus is free from such interaction. They also point out the possibility of the existence of such rotational isomers for the native Fe(II) systems, oxyHb and oxyMb, the perturbed $\nu(O_2)$ being inferred from Raman intensities and the free $\nu(O_2)$ being observed at 1156 cm^{-1} in the IR spectrum.[15] Very recently, these same workers (20) published the results of a thorough study of model compounds and proteins containing cobalt mesoporphyrin. These studies clearly provide support for their earlier interpretation, although the authors were careful to point out that ambiguities remained regarding the origin of the appearance of multiple, isotope-sensitive, bands in the ν(O–O) region.

It should be pointed out that the RR spectra of O_2 adducts of cobalt porphyrins in the 1000–1200 cm^{-1} region are often complicated by the presence of core vibrations of the macrocycle, axial ligand vibrations, and solvent bands. In an attempt to provide a better understanding of these complicated vibrational spectral patterns, we have undertaken a comprehensive study of a number of model compounds. Specifically, we have performed strategic isotopic labeling in order to demonstrate that certain multiplets arise from vibrational coupling and thus to distinguish this effect from other, steric or environmental, factors that may give rise to multiple bands. Such a clarification, coupled with careful and thorough studies of a number of porphyrins and axial ligands under a range of experimental conditions, can permit a more definitive interpretation of the effects of steric and environmental factors on the vibrational frequencies of the Co–O_2 linkage.

Experimental Section

Compound Preparation. The porphyrins used in this work were prepared according to standard procedures.[21] The $^2H_8$ and $^2H_{20}$ analogues of tetraphenylporphine (TPP) were prepared as previously described.[22] The picket-fence porphyrin complexes were purchased from Midcentury Chem Co. and used without further purification. Cobalt complexes of the other porphyrins were prepared by refluxing, under a nitrogen atmosphere, a solution of the porphyrin in chloroform to which was added a saturated solution of $Co(CH_3COO)_2{\cdot}4H_2O$ in methanol. After fluorescence had disappeared, the solution was cooled to room temperature, extracted with water (three times), and evaporated to dryness. The resulting solid was dissolved in a minimal volume of methylene chloride and chromatographed on alumina (Grade IV) with methylene chloride eluent. The nonfluorescent fractions were collected and evaporated to dryness and the resulting solid recrystallized from methylene chloride/heptane.[21] The nitrogenous bases that were used in this study were purified by distillation (liquids) or recrystallization and sublimation (solids). The sample of 2-methylimidazole-d_5 was prepared by heating a solution of 2 methylimidazole (1.0 g in 25 mL of ^2H_2O) in a sealed tube (100 mL total volume of tube) at 190 °C for 4 days. The tube was cooled and cautiously opened and the excess ^2H_2O removed by evaporation at reduced pressure. The sample was dissolved in 25 mL of methanol and evaporated. This was repeated several times to ensure complete exchange of the N–H proton to yield 2-methylimidazole-d_5. The solid sample was sublimed at 70 °C to yield pure white needles. Mass spectral analysis showed a parent ion peak of 87 amu with only small amounts of species with lower deuterium content.

Dichloromethane and chloroform were distilled from CaH_2 and toluene from sodium metal. Deuterated solvents and pyridine-d_5 were purchased from Aldrich Chemical Co. and Merck, Sharpe and Dome, Canada Ltd., and used as received. Samples of $^{16}O_2$ (prepurified, Matheson Gas Co.) and $^{18}O_2$ (ca. 99% pure, Monsanto Research) were used as received. The scrambled $^{16}O^{18}O$ was prepared by exposing a mixture of equivalent amounts of $^{16}O_2$ and $^{18}O_2$ to an electrical discharge from a Tesla coil. The final ratio of $^{16}O_2$:$^{16}O^{18}O$:$^{18}O_2$ was found to be ~1:2:1 as determined by Raman spectroscopy.

Spectral Measurements. The RR spectra were recorded on a Spex Model 1401 double monochromator equipped with a Spex DPC-2 digital photometer system. Excitation at 457.9 nm was made with a Spectra-Physics Model 164-08 Ar ion laser and that at 406.7 nm was by a

(6) Traylor, T. G. *Acc. Chem. Res.* **1981**, *14*, 102.
(7) Almog, J.; Baldwin, J. E.; Huff, J. *J. Am. Chem. Soc.* **1975**, *97*, 227.
(8) Linard, J. E.; Ellis, P. E.; Budge, J. R.; Jones, R. D.; Basolo, F. *J. Am. Chem. Soc.* **1980**, *102*, 1896.
(9) Ogoshi, H.; Sugimoto, H.; Yoshida, Z. *Heterocycles* **1975**, *3*, 1146.
(10) Momenteau, J.; Loock, B. *J. Mol. Catal.* **1980**, *7*, 315.
(11) (a) Barlow, C. H.; Maxwell, J. C.; Wallace, W. J.; Caughey, W. S. *Biochem. Biophys. Res. Commun.* **1973**, *55*, 91. (b) Maxwell, J. C.; Volpe, J. A.; Barlow, C. H.; Caughey, W. S. *Biochem. Biophys. Res. Commun.* **1974**, *58*, 166.
(12) Brunner, H. *Naturwissenshaften* **1974**, *61*, 129.
(13) Burke, J. M.; Kincaid, J. R.; Peters, S.; Gagne, R. R.; Collman, J. P.; Spiro, T. G. *J. Am. Chem. Soc.* **1978**, *100*, 6083.
(14) Collman, J. P.; Brauman, J. I.; Halbert, T. R.; Suslick, K. S. *Proc. Natl. Acad. Sci. U.S.A.* **1976**, *73*, 3333.
(15) Alben, J. O.; Bare, G. H.; Moh, P. P. In "Biochemical and Clinical Aspects of Hemoglobin Abnormalities"; Caughey, W. S., Ed.; Academic Press: New York, 1978; p 607.
(16) Walters, M. A.; Spiro, T. G. *Biochemistry* **1982**, *21*, 6989.
(17) Case, D. A.; Huynh, B. H.; Karplus, M. *J. Am. Chem. Soc.* **1979**, *101*, 4433.
(18) Tsubaki, M.; Yu, N. T. *Proc. Natl. Acad. Sci. U.S.A.* **1981**, *78*, 3581.
(19) Bajdor, K.; Nakamoto, K.; Kincaid, J. *J. Am. Chem. Soc.* **1983**, *105*, 678.
(20) Mackin, H. C.; Tsubaki, M.; Yu, N. T. *Biophys. J.* **1983**, *41*, 349.
(21) Smith, K. M. "Porphyrins and Metalloporphyrins"; Elsevier: Amsterdam, 1975.
(22) Burke, J. M.; Kincaid, J. R.; Spiro, T. G. *J. Am. Chem. Soc.* **1978**, *100*, 6077.

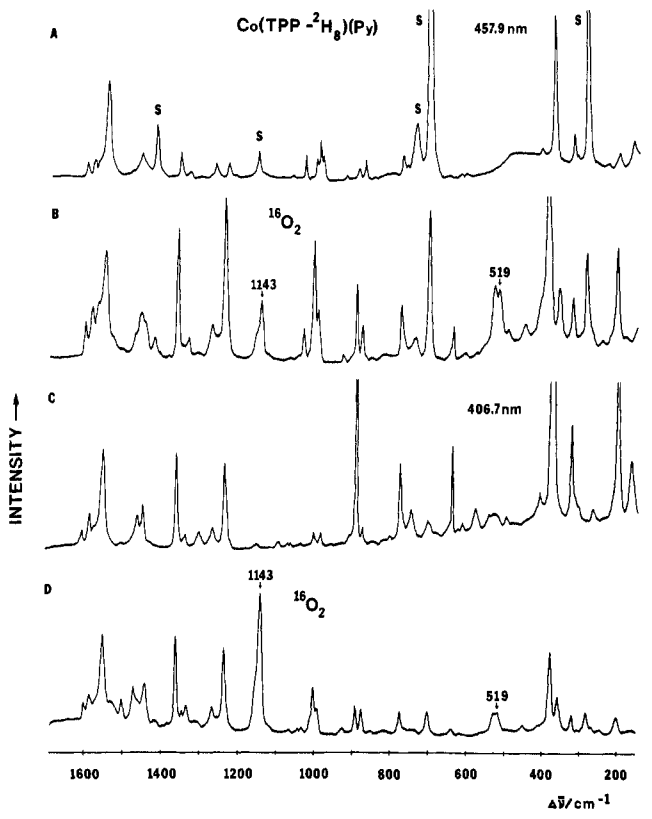

Figure 1. Resonance Raman spectra of Co(TPP-d_8) in CH_2Cl_2 solution containing 3% pyridine at ~−90 °C: (A) Co(TPP-d_8) + no oxygen, 457.9-nm excitation; (B) Co(TPP-d_8) + $^{16}O_2$ (~4 atm), 457.9-nm excitation; (C) Co(TPP-d_8) + no oxygen, 406.7-nm excitation; (D) Co(TPP-d_8) + py + $^{16}O_2$ (~4 atm), 406.7-nm excitation (S denotes the solvent band).

Spectra-Physics Model 164-01 Kr ion laser. A spectral band-pass of 4 cm^{-1} was used, and laser power was kept below 5 mW.

Preparation of the sample for spectral measurement was carried out as follows. A small amount of solid metalloporphyrin (less than 0.5 mg) was placed into a small glass bulb, which was then attached to a vacuum line. In those cases where the nitrogeneous base was a solid, the appropriate amount (30–50 equiv) was placed into the bulb before attaching it to the vacuum line. The solvent was degassed by three freeze–pump–thaw cycles and then transferred under vacuum to the sample bulb. The liquid nitrogeneous bases were degassed and transferred with the solvent. Oxygen was introduced by momentarily (less than 2 s) exposing the frozen sample to a vessel containing oxygen via vacuum line connection. At this point, the stem of the bulb was sealed at a distance approximately 1 cm above the body of the bulb that was immersed in liquid nitrogen. Caution! The bulb may explode at ambient temperature due to the high O_2 pressure (vide infra). Therefore, the sealed bulb is kept in liquid nitrogen until it is attached to the front edge of the copper tip that was then cooled to ~100 K by a CTI Model 21 closed cycle helium refrigerator. The pressure in the bulb was estimated to be ca. 4 atm assuming rapid pressure equilibration during the 2-s exposure time and knowledge of the volumes of the oxygen vessel, sample bulb, and connection lines. Approximate temperatures of the samples were estimated by the relative intensities of Stokes and anti-Stokes lines of solvent for several samples. Calibration of the frequency reading was made by using the solvent bands and estimated accuracy of the frequency reading was ±1 cm^{-1}.

Results

Co(TPP) and Co(TPP-d_8). Typical spectra over the entire frequency region of interest are shown in Figure 1. It is clear from the figure that the binding of $^{16}O_2$ gives rise to new bands at 1143 and 519 cm^{-1} that are shifted to 1084 and 498 cm^{-1}, respectively, by the $^{16}O_2$–$^{18}O_2$ substitution.[19] Thus, these two bands are reasonably assigned to the ν(O–O) and ν(CoO) of Co(TPP-d_8)(py)O_2, respectively. The observed frequencies in the ν(O–O) region for all of the complexes studied are listed in Table I along with sampling conditions and comments on items of special note. Figure 1 also shows that the ν(O–O) is greatly enhanced while

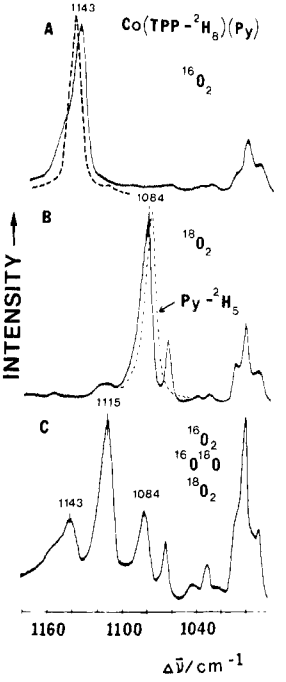

Figure 2. Resonance Raman spectra (406.7-nm excitation) of Co(TPP-d_8) dioxygen adducts in CH_2Cl_2 solution containing 3% pyridine at ~−90 °C under ~4 atm of O_2 pressure: (a) Co(TPP-d_8) + $^{16}O_2$, dotted line shows the position of ^{16}O–^{16}O in $C^2H_2Cl_2$ at 1148 cm^{-1}; (B) Co(TPP-d_8) + $^{18}O_2$, dotted line shows the fragment of the spectrum when py-d_5 has been used as a base instead of py (^{18}O–^{18}O at 1082 cm^{-1} with py-d_5); (C) Co(TPP-d_8) + $^{16}O_2$ + $2^{16}O^{18}O$ + $^{18}O_2$.

the ν(Co–O) does not change appreciably when the excitation line is changed from 457.9 to 406.7 nm.[19] Other spectral changes are noted upon oxygenation. However, they are insensitive to $^{18}O_2$ substitution; thus, these are not associated with the O_2 linkage and will not be discussed further in this paper. The d_8 analogue of TPP was used merely to avoid overlap of ν(^{18}O–^{18}O) with an internal model of Co(TPP) that occurs at 1080 cm^{-1}.[19]

Figure 2 shows the RR spectra of Co(TPP-d_8)(py)O_2 for $^{16}O_2$ and $^{18}O_2$ and a mixture of $^{16}O_2$, $^{16}O^{18}O$, and $^{18}O_2$ in the ν(O–O) region. The dotted line in trace B shows the spectrum obtained by using py-d_5. The ν(^{18}O–^{18}O) at 1084 cm^{-1} is shifted to 1082 cm^{-1} and the sideband at 1067 cm^{-1} disappears completely upon py-d_5 substitution. The side band at 1067 cm^{-1} appears for all porphyrins when their solutions containing py are saturated with $^{18}O_2$. This indicates vibrational interaction between ν(^{18}O–^{18}O) and an internal py mode at 1068 cm^{-1} (vide infra). In trace C, a symmetrical single band is observed at 1115 cm^{-1} for the $^{16}O^{18}O$ species whereas multiple bands are observed in the ν(^{16}O–^{16}O) and ν(^{18}O–^{18}O) regions.

Figure 3 shows the RR spectra of Co(TPP-d_8)(1,2-DiMeIm)$^{16}O_2$ and its $^{18}O_2$ analogue. It is noted that a clear doublet appears in the ν(^{16}O–^{16}O) region whereas a single peak is observed in the ν(^{18}O–^{18}O) region. Similar ν(^{16}O–^{16}O) frequencies were observed for Co(TPP) under the same experimental conditions (Table I).

Co(OEP) and Co(OEP-d_4). Figure 4 shows the RR spectra of Co(OEP-d_4)(py)O_2 for the $^{16}O_2$, $^{18}O_2$, and a mixture of $^{16}O_2$, $^{18}O_2$, and $^{16}O^{18}O$. The ν(O–O) are observed at 1145, 1082, and 1112 cm^{-1} for these isotopic oxygen molecules. The strong band at 1139 cm^{-1} in trace B is clearly due to an internal mode of OEP. Figure 4 also shows the spectra of these O_2 adducts in the ν(Co–O) region. The band at 521 cm^{-1} is shifted to 498 cm^{-1} by $^{16}O_2$–$^{18}O_2$ substitution. It is interesting to note that the two maxima observed for the $^{16}O_2$ and $^{18}O_2$ species are shifted closer to each other (by ~2 cm^{-1}) when the mixed isotopes are used so that their separation becomes smaller. Similar results were obtained for Co(OEP)(py)$^{16}O_2$ and its $^{18}O_2$ analogue (Table I).

Co(PPIXDME). Figure 5 shows the RR spectra of Co(PPIXDME)(py)$^{16}O_2$ and its $^{18}O_2$ analogue using 457.9-nm ex-

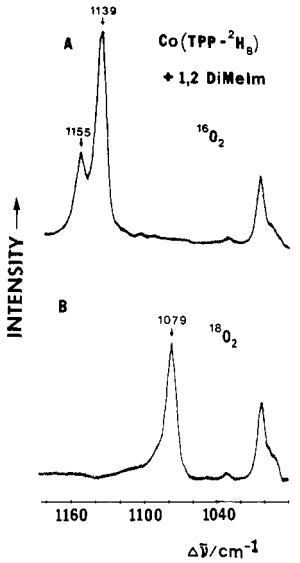

Figure 3. Resonance Raman spectra (406.7-nm excitation) of dioxygen adducts of Co(TPP-d_8) in CH_2Cl_2 containing 3% of 1,2-DiMeIm at ~−90 °C under ~4 atm of O_2 pressure: (A) Co(TPP-d_8) + $^{16}O_2$; (B) Co(TPP-d_8) + $^{18}O_2$.

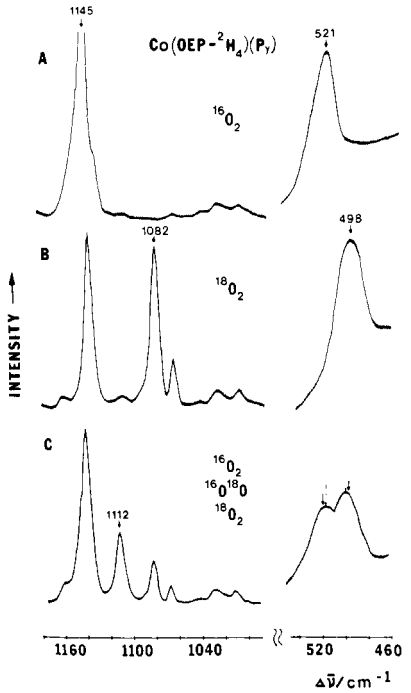

Figure 4. Resonance Raman spectra of dioxygen adducts of Co(OEP-d_4) in CH_2Cl_2 containing 3% of py at ~−90 °C under ~4 atm of O_2 pressure. In the ν(Co–O) region 457.9-nm excitation and in the ν(O–O) region 406.7-nm excitation have been used: (A) Co(OEP-d_4) + $^{16}O_2$; (B) Co(OEP-d_4) + $^{18}O_2$; (C) Co(OEP-d_4) + $^{16}O_2$ + $^{16}O^{18}O$ + $^{18}O_2$.

citation. Although the spectrum in the $\nu(^{16}O–^{16}O)$ region is rather complicated, it is possible to assign the $\nu(^{16}O–^{16}O)$ at 1143 cm^{-1} since only this band is shifted to 1083 cm^{-1} by $^{16}O_2$–$^{18}O_2$ substitution. The spectra in the ν(Co–O) region are simple; the ν(Co–O) at 513 cm^{-1} is shifted to 491 cm^{-1} upon $^{16}O_2$–$^{18}O_2$ substitution.

Co(T_{piv}PP). Figure 6 shows the RR spectra of Co(T_{piv}PP)(1,2-DiMeIm)$^{16}O_2$ and its $^{18}O_2$ and $^{16}O^{18}O$ analogues in the ν(O–O) region. A distinct doublet was observed at 1157 and 1143 cm^{-1} for the $^{16}O_2$ species in complete agreement with those data previously obtained by Yu and co-workers.[20] A slight asymmetric feature noted for the $\nu(^{18}O–^{18}O)$ band is due to overlap with an internal mode of the Co porphyrin at 1078 cm^{-1}. A strong single peak was observed at 1118 cm^{-1} for the $^{16}O^{18}O$ species with slight

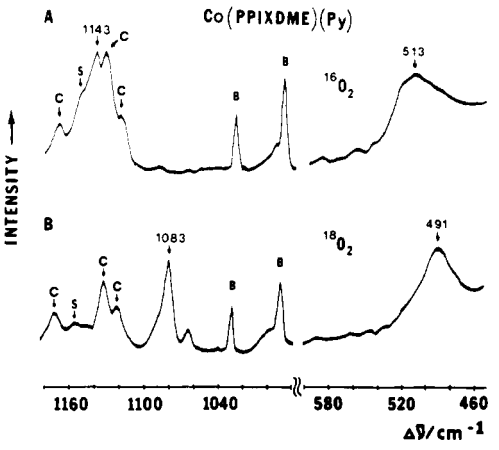

Figure 5. Resonance Raman spectra (457.9-nm excitation) of dioxygen adducts of Co(PPIXDME) in CH_2Cl_2 containing 3% pyridine at ~−90 °C under ~4 atm of O_2 pressure (S, C, and B denote solvent, complex (metalloporphyrin), and base (pyridine), respectively): (A) Co(PPIXDME) + $^{16}O_2$; (B) Co(PPIXDME) + $^{18}O_2$.

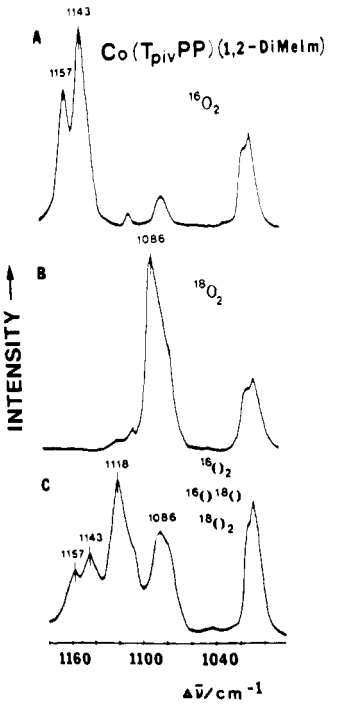

Figure 6. Resonance Raman spectra (406.7-nm excitation) of dioxygen adducts of Co(T_{piv}PP) in CH_2Cl_2 containing 3% 1,2-DiMeIm at ~−90 °C under ~4 atm of O_2 pressure: (A) Co(T_{piv}PP) + $^{16}O_2$; (B) Co(T_{piv}PP) + $^{18}O_2$; (C) Co(T_{piv}PP) + $^{16}O_2$ + $^{16}O^{18}O$ + $^{18}O_2$.

asymmetry due to the presence of another Co porphyrin band at 1105 cm^{-1}.

Figure 7 shows the RR spectra of Co(T_{piv}PP)(base)$^{16}O_2$ for a variety of base ligands. The dotted line in trace A illustrates the spectrum of the corresponding $^{18}O_2$ species in which a single peak at 1083 cm^{-1} with slight asymmetry is noted as for the 1,2-DiMeIm species (Figure 6). In the case of 2-substituted bases such as 2-pic and 2-Brpy, only single broad bands were observed. This is in contrast to the case of 4-pic or py that have no substituents at the 2-position and show single, rather sharp, bands.

Discussion

Origin of Multiple Bands in the ν(O–O) Region. As can be seen in Figure 3, 6, and 7, the $\nu(^{16}O–^{16}O)$ bands near 1150 cm^{-1} split into two distinct bands when the base ligand is 1,2-DiMeIm and 2-MeIm and are broadened considerably when the base is 2-pic or 2-Brpy. However, no splitting is observed when the base is py or 4-pic. Similar splitting of the $\nu(^{18}O–^{18}O)$ band is observed near 1080 cm^{-1} for Co(TPP-d_8) (Figure 2), Co(OEP-d_4) (Figure 4),

Table I. Observed Frequencies

porphyrin	base	solvent	$\nu(^{16}O_2)$	$\nu(^{18}O_2)$	$\nu(^{16}O-^{18}O)$
Co(TPP-d_8)	py	CH_2Cl_2	1143 (1155)[c]	1084 (1067)	1115
	py-d_5	CH_2Cl_2	1144 (1155)	1082	
	py	$C^2H_2Cl_2$	1148		
	py-d_5	$C^2H_2Cl_2$		1083	
	py	toluene	1160 (1150)	1094 (1067)	
	py-d_5	toluene + 20% MeOH		1089	
	py	toluene-d_8	1159[a]		
	4-CNpy	toluene	1166 (1153)	1101	
	2-MeIm	CH_2Cl_2	1146, 1159		
	1,2-DiMeIm	CH_2Cl_2	1155, 1139	1079	
	1-MeIm	CH_2Cl_2	1143 (1155)	1073 (1094)	
	1-MeIm	$C^2H_2Cl_2$	1147		
	1-MeIm	toluene	1148 (1155)	1075 (1094)	
	n-Bu amine	toluene	1143 (1155)		
Co(TPP-d_{20})	py	CH_2Cl_2	1143 (1155)		
Co(TPP)	py	CH_2Cl_2	1143 (1155)	1084 (1067)	
	py	toluene	1160 (1150)		
	1-MeIm	CH_2Cl_2	1144 (1155)		
	n-Bu amine	CH_2Cl_2	1139 (1155)		
	py	CH_2Cl_2 + 20% MeOH	1140 (1155)		
	$P(Ph)_3$	CH_2Cl_2	1138 (1155)		
Co(OEP)	py	CH_2Cl_2	1145	1082 (1067)	1112
	1,2-DiMeIm	CH_2Cl_2	1144, 1158	1078	
Co(OEP-d_4)	py	CH_2Cl_2	1145	1082 (1067)	1112
Co(PPIXDME)[b]	py	CH_2Cl_2	1143	1083 (1067)	
Co(DFDPDME)[b]	py	CH_2Cl_2	1143	1085 (1067)	
Co(TpivPP)	py	CH_2Cl_2	1151		
	py	toluene	1154		
	4-pic	CH_2Cl_2	1150		
	2-pic	CH_2Cl_2	1161 (br)		
	2-Brpy	CH_2Cl_2	(1155), 1172 (br)		
	2-EtIm	CH_2Cl_2	1149 (br, asym)		
	1,2-DiMeIm	CH_2Cl_2	1157, 1143	1086	1118
	2-MeIm	CH_2Cl_2	1160, 1145	1084	
	2-MeIm-d_5	CH_2Cl_2	1155 (slight broadening)		
	imidazole (Im)	CH_2Cl_2	1151 (weak shoulders at 1161, 1139 cm^{-1})		

[a] Very weak shoulders at 1147 and 1176 cm^{-1}. [b] 457.9-nm excitation. [c] Brackets indicate that the band is a shoulder or minor band.

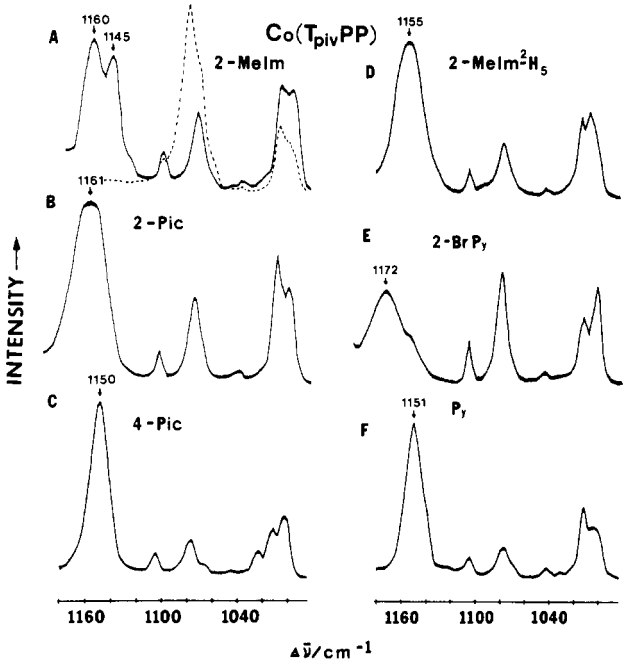

Figure 7. Resonance Raman spectra (406.7-nm excitation) of dioxygen adducts of Co(T_{piv}PP) in CH_2Cl_2 containing 3% of a variety of different bases at ~−90 °C under ~4 atm of $^{16}O_2$ pressure: (A) Co(T_{piv}PP) + 2-MeIm, dotted line shows the spectrum when $^{18}O_2$ is used; (B) Co(T_{piv}PP) + 2-Pic (picoline); (C) Co(T_{piv}PP) + 4-Pic (picoline); (D) Co(T_{piv}PP) + 2-MeIm-d_5; (E) Co(T_{piv}PP) + 2-Brpy (pyridine); (F) Co(T_{piv}PP) + py (pyridine).

Co(PPIXDME) (Figure 5), and all other Co porphyrins when py serves as a fifth ligand.

The splitting observed for sterically hindered bases mentioned above has been previously noted by Yu and co-workers[20] and was reasonably interpreted as being suggestive of the presence of two different conformers. However, for all complexes with these bands, the separation between the doublet bands in the $\nu(^{16}O-^{16}O)$ region is 15–20 cm^{-1}. If these frequencies arise due to the presence of two conformers (or any type of isomers), it must be expected that the $\nu(^{18}O-^{18}O)$ region should also exhibit two bands separated by a comparable difference in frequency and having relative intensities similar to those observed in the $\nu(^{16}O-^{16}O)$ region. Such is not the case; only one symmetric band is observed in the $\nu(^{18}O-^{18}O)$ region (Figure 3). The slight asymmetry observed for this band in Figure 6 is very likely due to the presence of a porphyrin band near 1078 cm^{-1}. A completely symmetric $\nu(^{18}O-^{18}O)$ band was also observed for Co(OEP)(1,2-DiMeIm)$^{18}O_2$ (not shown).

The absence of a doublet in the $\nu(^{18}O-^{18}O)$ region having a separation comparable to that in the $\nu(^{16}O-^{16}O)$ region suggests a vibrational coupling mechanism as the origin of the splitting in the latter region. Several possibilities must be considered for such coupling. The most commonly encountered type is that known as Fermi resonance[23] in which there is an interaction between a fundamental vibration and an overtone or combination mode that is close in frequency and is of the same symmetry. For this type of interaction, the nonfundamental mode gains intensity at the expense of the fundamental and shifts of the frequencies of both modes from their inherent, nonperturbed, frequencies are observed. Such an interaction has been proposed for the native protein systems in which the first overtone of ν(Fe–O) at 567 cm^{-1} ($2 \times 567 = 1134$ cm^{-1}) is obviously in close proximity to $\nu(^{16}O-^{16}O)$ of these systems.[15] Such an interaction is very unlikely in the case of the cobalt systems, however, since the first overtone of the ν(Co–O) fundamental would occur at ~1040 cm^{-1}, a value too low to invoke Fermi resonance with the ~1150 cm^{-1} $\nu(^{16}O-^{16}O)$.

Table II. Vibrational Frequencies (cm^{-1}) of Axial Bases

		Pyridine Derivatives[a]	
pyridine	1148	2-bromopyridine	1144
2-picoline	1147	4-picoline	1220
		Imidazole Derivatives[b]	
imidazole	1135	1,2-dimethylimidazole	~1150
2-methyl-imidazole	~1150	1-methylimidazole	no bands between 1120 and 1200 cm^{-1}

[a] Reference 36. [b] References 37 and 38.

It is also unlikely that the splitting results from Fermi resonance between $\nu(^{16}O-^{16}O)$ and an overtone or combination mode of the porphyrin macrocycle because in those situations in which splitting is observed, it does not disappear by changing the porphyrin type (i.e., Co(OEP), Co(TPP), and Co(T_{piv}PP) all show splitting with 1,2-DiMeIm as the axial ligand). Such behavior also makes it less likely that the doublet originates from interaction between $\nu(^{16}O-^{16}O)$ and a fundamental macrocycle mode via the type of resonance interaction described previously.[20]

In fact, consideration of the data presented here, in which splitting or broadening is observed for all cobalt porphyrin derivatives where particular axial ligands (1,2-DiMeIm, 2-MeIm, 2-pic, 2-Brpy) are employed, would seem to indicate that the coupling involves internal modes (either fundamentals or nonfundamentals) of the axial ligand. The existence of this type of vibrational coupling is most clearly demonstrated by the spectra shown in Figure 2B. The solid line shows that a weaker band is observed at 1067 cm^{-1}, along with the stronger $\nu(^{18}O-^{18}O)$ at 1084 cm^{-1}, in a CH_2Cl_2 solution containing Co(TPP-d_8), pyridine, and $^{18}O_2$. The dotted line shows that the substitution of pyridine-d_5 for pyridine, keeping all other conditions constant, results in the disappearance of the 1067 cm^{-1} band and a slight shift of the $\nu(^{18}O-^{18}O)$ to 1082 cm^{-1} upon elimination of the vibrational coupling. The 1067 cm^{-1} band is a totally symmetric internal mode of pyridine which is shifted to 824 cm^{-1} upon perdeuteration.[24] This band is not observed when $^{16}O_2$ is employed (Figure 2A). It gains intensity only as a consequence of its proximity to a resonance enhanced band ($\nu(^{18}O-^{18}O)$) of the complex. This weak vibrational coupling is further supported by the 2 cm^{-1} downshift of the 1084 cm^{-1} band when pyridine-d_5 is employed.

We have also observed enhancement of a similar type when 4-CNpy is employed as the axial ligand in conjunction with $^{18}O_2$ (Table I). In this case the frequencies are relatively well separated (1101 and 1066 cm^{-1}), yet enhancement of the ligand band is evident. Apparently, intensity increase in the latter band is significant even though the $\nu(O-O)$ occurs at ~1100 cm^{-1}. This observation is consistent with the increased intensity of the 1067 cm^{-1} band relative to the $\nu(^{18}O-^{18}O)$ in the mixed isotope experiment since additional intensity is gained via the interaction between the pyridine mode (1067 cm^{-1}) and $\nu(^{16}O-^{18}O)$ (1115 cm^{-1}).

A similar type of interaction can be invoked to explain the doublets observed in the $\nu(^{16}O-^{16}O)$ region for the complexes mentioned above (Figures 3, 6, and 7). This explanation is strongly supported by the spectra shown in parts A and D Figures 7. As can be seen (Figure 7A), two distinct bands are observed at 1160 and 1145 cm^{-1}. Clearly, this doublet collapses to a single band upon substitution of 2-MeIm-d_5 (Figure 7D). That is, to the extent that 2-MeIm-d_5 is chemically equivalent to 2-MeIm (which is nearly certain, especially in that the N_1–H proton has been retained), the appearance of a single band in Figure 7D must be ascribed to the alteration of vibrational coupling.

It seems worthwhile to point out that in cases where splitting or broadening has been observed, the axial ligand of interest possesses a vibrational mode in the 1150 cm^{-1} region (Table II). In the cases of *N*-MeIm and 4-pic there does not exist a fundamental in this region and doublets are not observed. Although pyridine also possesses a band in this region (Table II), it does not correspond to a totally symmetric mode[24] and no splitting is observed as can be seen by the dotted line in Figure 2A.

To summarize this section, the behavior observed upon manipulation of vibrational frequencies via specific deuteration is consistent with the proposal that the $\nu(O_2)$ may couple with internal modes of the axial ligand. Apparently, this coupling does not result in large changes in the form of the internal modes of the axial ligands since the observed frequencies are not significantly different from those of the free ligand. That is, alterations in the composition of the internal modes as $^{18}O_2$ is substituted for $^{16}O_2$ are not extensive. This is also evident from consideration of the observed frequencies of $\nu(^{16}O-^{16}O)$ and $\nu(^{18}O-^{18}O)$ which indicate that the bound dioxygen closely resembles the behavior of a simple harmonic oscillator (vide infra).

Environmental Effects. Apparently the immediate environment of the Co–O_2 moiety may significantly influence the $\nu(O-O)$ frequency. As will be shown below, relatively large shifts are observed merely by changing the solvent. However, in order to evaluate this effect, it is first necessary to eliminate factors that may alter the inherent frequency of the $\nu(O-O)$ mode. In so doing we present evidence for a peculiar type of vibrational coupling between the $\nu(O-O)$ and an internal mode of surrounding solvent molecules. As can be seen in Figure 2, the 1143 cm^{-1} band exhibits a definite asymmetry, having a high-frequency shoulder at ~1155 cm^{-1}. The solvent used for this case was CH_2Cl_2, which has an internal mode at ~1156 cm^{-1}. On the other hand, if $C^2H_2Cl_2$ is used (all other conditions remaining the same) this asymmetry disappears and, most significantly, the $\nu(^{16}O-^{16}O)$ is now observed at 1148 cm^{-1} (dotted line, Figure 2A). It is noted that changing the solvent from CH_2Cl_2 to $C^2H_2Cl_2$ has no effect on $\nu(^{18}O-^{18}O)$, as can be seen in Table I. Such behavior implies the presence of vibrational coupling between $\nu(^{16}O-^{16}O)$ and an internal mode of CH_2Cl_2 that perturbs the $\nu(^{16}O-^{16}O)$ from its inherent value of 1148 cm^{-1}. Further support for this type of interaction is derived from considerations of separations between $\nu(O-O)$ bands in experiments with scrambled isotopes of O_2 (vide infra).

As can be seen in Table I, if toluene is used as the solvent the $\nu(^{16}O-^{16}O)$ is observed as a doublet having peaks at 1160 and 1150 cm^{-1}, whereas only one band is observed (1094 cm^{-1}) in the case of $^{18}O_2$. The 1150 cm^{-1} feature corresponds to an internal mode of toluene and disappears when toluene-d_8 is employed. Only a 1 cm^{-1} shift of the $\nu(O-O)$ (1160 → 1159 cm^{-1}) is observed when toluene-d_8 is used.

The apparent solvent effect is approximately 12 cm^{-1} (1160 → 1148 cm^{-1}) when comparing the frequencies in toluene and $C^2H_2Cl_2$. An identical value is obtained by comparing the corresponding $\nu(^{18}O-^{18}O)$ frequencies (1094 → 1082 cm^{-1} = 12 cm^{-1}). The 1082 cm^{-1} is taken from the data for the pyridine-d_5 case where the $\nu(^{18}O-^{18}O)$ is not perturbed by the internal pyridine mode. This 12 cm^{-1} downshift in methylene chloride relative to its value in toluene represents a strengthening of the Co–O bonding and corresponding weakening of the O–O bond, presumably via greater stabilization of the charge separation implied in the $Co^{\delta+}-O_2^{\delta-}$ formulation.[25]

Hydrogen bonding to the bound O_2 is considered to be an important feature in the native protein systems (vide infra).[18,26,27] In order to evaluate the effect of hydrogen bonding on $\nu(O-O)$ frequencies, we have carried out an experiment in which methanol (MeOH) was added to the system. As can be seen from the data presented in Table I, addition of 20% MeOH to a toluene solution of Co(TPP-d_8) induces a 5 cm^{-1} shift to lower frequency. This shift of $\nu(O-O)$ to lower frequency again implies a stabilization based on the $Co^{\delta+}-O_2^{\delta-}$ formulation, in this case presumably by hydrogen bonding to the terminal oxygen atom. It should be pointed out that in corresponding experiments using CH_2Cl_2, where charge separation is already stabilized to some degree by solvent molecules, the addition of 20% MeOH induced a slightly smaller

(23) Herzberg, G. "Molecular Spectra and Molecular Structure, II"; Van Nostrand: New York, 1945; p 215.
(24) Stidham, H. D.; DiLella, D. P. *J. Raman Spectrosc.* **1980**, *9*, 247.
(25) Stynes, H. D.; Ibers, J. A. *J. Am. Chem. Soc.* **1972**, *94*, 5125.
(26) Phillips, S. E. V.; Schoenborn, B. P. *Nature (London)* **1981**, *292*, 81.
(27) Kitagawa, T.; Ondrias, M. R.; Rousseau, D. L.; Ikeda-Saito, M.; Yonetoni, T. *Nature (London)* **1982**, *298*, 869.

shift in ν(O–O) (1143 → 1140 cm^{-1} for Co(TPP)).

The above results indicate that the bound O_2 may be stabilized by interaction with external solvent molecules. It is therefore interesting to note that such effects are evidently minimized in those cases where the O_2 moiety may be considered to be shielded. Thus, no such drastic solvent effects are observed for the picket-fence derivatives. As can be seen from the data presented in Table I, the $\nu(^{16}O–^{16}O)$ is observed at 1154 cm^{-1} in toluene, whereas it shifts only slightly (1151 cm^{-1}) in CH_2Cl_2. It is also noteworthy that in the latter case no asymmetry is exhibited (Figure 7F), in contrast to the situation where the O_2 moiety is exposed to the CH_2Cl_2 solvent molecules (Figure 2A) although such asymmetry, if present, may be difficult to detect considering the instrumental conditions used for these experiments.

The $\nu(O_2)$ for the picket-fence derivatives are observed at lower frequencies (~1154 cm^{-1}) than those for unprotected O_2 in complexes with other porphyrins in toluene (e.g., 1159 cm^{-1} in the case of CoTTP-d_8 in toluene-d_8). Such shifts may indicate the presence of some interaction which stabilizes the Co–O_2 moiety, perhaps weak hydrogen bonding to the amide groups in the "picket" linkage.[28]

Axial Ligand and Porphyrin Substituent Effects. Kinetic and equilibrium measurements of O_2 binding to a series of hemes with various bases indicate that binding is sensitive to the electron density at the metal center as expected on the basis of the $Co^{\delta+}–O_2^{\delta-}$ formulation.[6,29,30] As can be seen from Table I, the ν(O–O) is sensitive to variation of the axial ligand. For example, ν(O–O) shifts from 1166 cm^{-1} for the 4-cyanopyridine complex to 1143 cm^{-1} when *n*-butylamine serves as the axial ligand (using toluene as solvent). It should be pointed out that the apparent effect of axial ligand basicity on ν(O–O) is much reduced when CH_2Cl_2 is used as solvent, a masking effect similar to that observed in the experiments with methanol. Such an effect may also be partially responsible for the apparent lack of sensitivity of ν(O–O) to porphyrin substituent variation.

Utility of "Mixed-Isotope" Experiments. In addition to the utility of scrambled isotope experiments for investigation of the geometry of the Co–O_2 linkage,[31-33] such experiments also provide a sensitive probe for the detection of vibrational coupling between ν(O–O) and other modes. For the case of a diatomic molecule treated as a simple harmonic oscillator, the frequency of $\nu(^{16}O–^{18}O)$ must occur at precisely the average of the frequencies for $\nu(^{16}O–^{16}O)$ and $\nu(^{18}O–^{18}O)$ in the absence of any perturbations due to vibrational coupling. In the case of "end-on" bonding, if splitting of $\nu(^{16}O–^{18}O)$ is observed, then the average of these two frequencies would be precisely the average of the $\nu(^{16}O–^{16}O)$ and $\nu(^{18}O–^{18}O)$ frequencies.

For a value of $\nu(^{16}O–^{16}O)$ of ~1150 cm^{-1}, the $\nu(^{18}O–^{18}O)$ is expected to occur at 1084 cm^{-1}, a shift of ~66 cm^{-1}. Thus, ideally, the present experiment with scrambled isotope should produce three bands associated with $\nu(O_2)$ having a $\Delta\nu(^{16}O_2 \rightarrow {}^{18}O_2)$ of ~66 cm^{-1} and separations of ~33 cm^{-1} between $\nu(^{16}O_2)$ and $\nu(^{16}O–^{18}O)$ and between $\nu(^{16}O–^{18}O)$ and $\nu(^{18}O_2)$. The fact that the oxygen molecule is not free but is bound to the complex may lower the $\Delta\nu(^{16}O_2 \rightarrow {}^{18}O_2)$ slightly (~64–66 cm^{-1} shifts), but still the $\nu(^{16}O–^{18}O)$ frequency is expected to occur at the average of $\nu(^{16}O_2)$ and $\nu(^{18}O_2)$.

Any deviation from this type of pattern is an indication that one or more of the $\nu(O_2)$ are perturbed by vibrational interaction. In the present work, the spectra shown in Figure 2 provide a particularly clear demonstration of these effects. The apparent $\Delta\nu(^{16}O_2 \rightarrow {}^{18}O_2)$ is only 59 cm^{-1} (1143 → 1084 cm^{-1}), while $\Delta\nu(^{16}O_2 \rightarrow {}^{16}O^{18}O) = 28$ cm^{-1} and $\Delta\nu(^{16}O^{18}O \rightarrow {}^{18}O_2) = 31$ cm^{-1}. Earlier, it was shown that the actual $\nu(^{18}O–^{18}O)$ occurs at 1082 cm^{-1} upon removal of the vibrational coupling with pyridine (dotted line in Figure 2B). Similarly, the inherent frequency of $\nu(^{16}O–^{16}O)$ is seen to be 1148 cm^{-1} upon removal of the perturbation by CH_2Cl_2 (dotted line in Figure 2A). Thus, the actual behavior of the $\nu(O_2)$ frequencies in this system conforms with expectations, giving a $\Delta\nu(^{16}O_2 \rightarrow {}^{18}O_2) = 66$ cm^{-1} with the frequency of the $\nu(^{16}O–^{18}O)$ band occurring at precisely the average of the frequencies of $\nu(^{16}O_2)$ and $\nu(^{18}O_2)$.

Similar considerations of the case of 1,2-DiMeIm complexes with Co(T_{piv}PP) (Figure 6) indicate that the $\nu(^{16}O–^{16}O)$ is coupled to another mode. Thus, on the basis of a 32 cm^{-1} difference between $\nu(^{16}O–^{18}O)$ at 1118 cm^{-1} and $\nu(^{18}O–^{18}O)$ at 1086 cm^{-1}, a $\nu(^{16}O–^{16}O)$ frequency of 1150 cm^{-1} is predicted, a value equal to the average of the frequencies of the components of the doublet observed at 1157 and 1143 cm^{-1}. In the 1-MeIm complexes, interaction of $\nu(^{18}O–^{18}O)$ with an internal mode of the ligand (1080 cm^{-1}) gives rise to anomously low frequencies of 1073–1075 cm^{-1} (Table I and ref 20).

Implications for Oxygen Complexes of Heme Proteins. The studies reported here demonstrate the considerably complex behavior of the vibrational frequencies of bound O_2 and confirm that, as Yu and co-workers have postulated,[18,20] the $\nu(O_2)$ may couple with other modes. In these previous reports, Yu and co-workers suggested the possibility that two types of bound oxygen may be present in heme proteins, one exhibiting an unperturbed $\nu(O_2)$ at ~1153 cm^{-1} and the other a vibrationally coupled $\nu(O_2)$ at ~1122 cm^{-1}. Although our results suggest that the vibrational coupling may involve internal modes of the axial ligand rather than the porphyrin, they support the proposal of these workers that the lower frequency band may be ascribed to the presence of interactions of the bound O_2 with distal residues. This latter point is indirectly supported by our data in the following sense.

We have observed no dramatic effects of axial ligand basicity, steric constraints, or substituent variation. Thus, $\nu(O_2)$ is apparently only weakly sensitive to variation of electron density at the cobalt ion. In the proteins, electron density at the cobalt ion may be controlled by modulation of proximal histidine basicity through hydrogen bonding with the protein backbone,[34] by tension in the Co–N(proximal histidine) bond, or, possibly, by rotation of vinyl groups on the macrocycle periphery as a result of steric interactions with residues in the heme pocket.[35] Our data indicate that the ν(O–O) is not sufficiently sensitive to such factors to reflect changes of the magnitude which might be expected to occur in the protein. However, it is very sensitive to interactions with solvent molecules that can stabilize the ($Co^{\delta+}–O_2^{\delta-}$) charge separation. Thus, the lower frequency component of $\nu(O_2)$ in the protein spectra may correspond to a species in which the bound oxygen interacts with a distal residue such as the N–H group of the distal histidine.[36,37]

Our data represent only a limited number of complexes and thus provide only a qualitative estimate of the importance of these types of interactions. Future studies, involving a larger number of additives covering a wide range of hydrogen bonding capabilities, may provide a more reliable estimate of the importance of such distal hydrogen bonding in the protein systems.

Acknowledgment. This work was supported by grants from The Research Corp. (J.R.K.), the National Institutes of Health (AM/HL 32318-01, J.R.K.), and the National Science Foundation (PCM8114676, CHE8205522, K.N. and K.B.). We wish to thank Professor Yu for providing results of his investigations prior to their publication.

(28) Momenteau, M.; Lavalette, D. *J. Chem. Soc., Chem. Commun.* **1982**, 341.
(29) Traylor, T. G.; White, D. K.; Campbell, D. H.; Berzinis, A. P. *J. Am. Chem. Soc.* **1981**, *103*, 4932.
(30) Jones, R. D.; Budge, J. R.; Ellis, P. E.; Linard, J. E.; Summerville, D. A.; Basolo, F. *J. Organomet. Chem.* **1979**, *181*, 151.
(31) Watanabe, T.; Ama, S.; Nakamoto, K. *J. Phys. Chem.* **1984**, *88*, 440.
(32) Rodley, G. A.; Robinson, W. T. *Nature (London)* **1972**, *235*, 438.
(33) Duff, L. L.; Appelman, E. H., Shriver, D. F.; Klotz, I. M. *Biochem. Biophys. Res. Commun.* **1979**, *90*, 1098.
(34) Valentine, J. S.; Sheridan, R. P.; Allen, L. C.; Khan, P. C. *Proc. Natl. Acad. Sci. U.S.A.* **1979**, *76*, 1009.
(35) Warshel, A.; Weiss, R. *J. Am. Chem. Soc.* **1981**, *103*, 446.
(36) Shindo, E. In "Infrared Absorption Spectra"; Nankodo: Tokyo, 1958; Vol. 3, p 163.
(37) Dollish, F. R.; Fateley, W. G.; Bentley, F. F. "Characteristic Raman Frequencies of Organic Compounds"; Wiley: New York, 1974; p 230.
(38) Bouchert, J., Aldrich Library of Infrared Spectra, Aldrich Chemical Co., 1970.